AMERICAN SOCIETY FOR MICROBIOLOGY | Journal of Bacteriology®

RESEARCH ARTICLE

SwsB and SafA Are Required for CwlJ-Dependent Spore Germination in *Bacillus subtilis*

Jeremy D. Amon,[a] Akhilesh K. Yadav,[b,c] Fernando H. Ramirez-Guadiana,[a] Alexander J. Meeske,[a] Felipe Cava,[b] David Z. Rudner[a]

[a]Department of Microbiology, Harvard Medical School, Boston, Massachusetts, USA
[b]Laboratory for Molecular Infection Medicine, Department of Molecular Biology, Umeå University, Umeå, Sweden
[c]Analytical Chemistry Division, CSIR-Indian Institute of Toxicology Research, Lucknow, India

ABSTRACT When *Bacillus subtilis* spores detect nutrients, they exit dormancy through the processes of germination and outgrowth. A key step in germination is the activation of two functionally redundant cell wall hydrolases (SleB and CwlJ) that degrade the specialized cortex peptidoglycan that surrounds the spore. How these enzymes are regulated remains poorly understood. To identify additional factors that affect their activity, we used transposon sequencing to screen for synthetic germination defects in spores lacking SleB or CwlJ. Other than the previously characterized protein YpeB, no additional factors were found to be specifically required for SleB activity. In contrast, our screen identified SafA and YlxY (renamed SwsB) in addition to the known factors GerQ and CotE as proteins required for CwlJ function. SafA is a member of the spore's proteinaceous coat and we show that, like GerQ and CotE, it is required for accumulation and retention of CwlJ in the dormant spore. SwsB is broadly conserved among spore formers, and we show that it is required for CwlJ to efficiently degrade the cortex during germination. Intriguingly, SwsB resembles polysaccharide deacetylases, and its putative catalytic residues are required for its role in germination. However, we find no chemical signature of its activity on the spore cortex or *in vitro*. While the precise, mechanistic role of SwsB remains unknown, we explore and discuss potential activities.

IMPORTANCE Spore formation in *Bacillus subtilis* has been studied for over half a century, and virtually every step in this developmental process has been characterized in molecular detail. In contrast, how spores exit dormancy remains less well understood. A key step in germination is the degradation of the specialized cell wall surrounding the spore called the cortex. Two enzymes (SleB and CwlJ) specifically target this protective layer, but how they are regulated and whether additional factors promote their activity are unknown. Here, we identified the coat protein SafA and a conserved but uncharacterized protein YlxY as additional factors required for CwlJ-dependent degradation of the cortex. Our analysis provides a more complete picture of this essential step in the exit from dormancy.

KEYWORDS sporulation, germination, cortex lytic enzymes, deacetylase, sporulation

In response to starvation, *Bacillus subtilis* differentiates into metabolically inactive and highly resilient endospores (here referred to as "spores") (1, 2). Spores can remain metabolically inactive for decades and yet upon exposure to nutrients will rapidly exit dormancy and resume vegetative growth (3). The process of spore formation has been extensively studied for over 50 years, and virtually all of the factors required for this morphological process have been identified (1, 2, 4, 5). In many cases, biochemical activities and pathways in which these factors act have been defined in molecular

Citation Amon JD, Yadav AK, Ramirez-Guadiana FH, Meeske AJ, Cava F, Rudner DZ. 2020. SwsB and SafA are required for CwlJ-dependent spore germination in *Bacillus subtilis*. J Bacteriol 202:e00668-19. https://doi.org/10.1128/JB.00668-19.

Editor Tina M. Henkin, Ohio State University

Address correspondence to David Z. Rudner, david_rudner@hms.harvard.edu.

Received 23 October 2019
Accepted 13 December 2019
Accepted manuscript posted online 23 December 2019
Published 25 February 2020

terms. In contrast, significantly less is known about germination and outgrowth of the dormant spore (6–8).

The dormant spore is composed of a dehydrated core surrounded by several protective layers. The core contains a highly compacted chromosome, ribosomes, tRNAs, and proteins and small molecules deposited during spore formation. Some of these factors provide resistance during dormancy, while others promote germination and outgrowth (9–11). A calcium chelate of dipicolinic acid (Ca^{2+}-DPA) is present in very high concentrations in the core, and its accumulation during sporulation contributes to water displacement (12). The core is surrounded by a lipid bilayer called the inner spore membrane, and this in turn is surrounded by two distinct layers of peptidoglycan (PG) (13). The inner PG layer, called the germ cell wall, resembles vegetative PG and serves as the nascent cell wall during outgrowth (14). The outer PG layer is called the cortex. The cortex is highly enzymatically modified with ~50% of its *N*-acetyl muramic acid (MurNAc) residues converted to muramic delta-lactam residues (15–17). The cortex plays a key role in spore dehydration by physically constraining the core and preventing its expansion. The cortex is surrounded by a second lipid bilayer called the outer spore membrane that is thought to be at least partially permeabilized. This bilayer is itself surrounded by a highly cross-linked proteinaceous coat composed of >70 proteins that form morphologically distinct inner and outer coat layers (18). Other endospore-forming bacteria have additional layers surrounding the coat, including glycosylated protein layers called the crust and the exosporium (19).

In response to specific nutrients—typically amino acids, sugars, or purine nucleosides—dormant spores initiate germination (20). Once triggered, spore germination follows a well-documented series of chemical and physical events starting with the release of monovalent ions from the spore core (21). This is followed by the excretion of the large stores of Ca^{2+}-DPA (22) and partial rehydration of the core. Next, two cortex lytic enzymes, SleB and CwlJ, are activated. The activation of these enzymes is critical for germination and outgrowth—without the activity of at least one of the two, the cortex remains undigested, and the core remains physically constrained and incompletely hydrated (23, 24). Degradation of the cortex allows for expansion of the core and complete rehydration, which enable the resumption of metabolic activity and synthesis of macromolecules. Finally, core swelling and possibly protease activity lead to mechanical breakage of the coat and outgrowth of the now-vegetative cell.

SleB and CwlJ are functionally redundant. Both enzymes specifically recognize the muramic delta-lactam residues in the glycan chains of the cortex and thus specifically degrade the cortex layer while leaving the germ cell wall intact (23, 25, 26). However, they differ in their localizations and mechanisms of activation. SleB is a secreted lytic transglycosylase that is produced in the developing spore and is held at or near the inner membrane (27). CwlJ is produced in the mother cell and is deposited in the spore coat (28). Accordingly, upon activation, these enzymes are thought to degrade the cortex from opposite sides: SleB works from the inside out, and CwlJ works from the outside in. An integral membrane protein, YpeB, is required for SleB accumulation in the spore and has been hypothesized to participate in maintaining SleB in an inactive state (29–31). However, this has not been experimentally verified, and the mechanism by which inhibition is relieved during germination is unknown. Similarly, the coat protein GerQ is required for CwlJ accumulation in the spore (32). Interestingly, Ca^{2+}-DPA is required for CwlJ activity; thus, excretion of this small molecule from the spore core is thought to function as an autocrine signal to initiate CwlJ-dependent cortex degradation (33). However, whether Ca^{2+}-DPA activates CwlJ directly or indirectly remains unknown.

Thus, although the morphological steps required to exit dormancy and resume vegetative growth are well defined and several of the proteins involved are known, how these factors function at the molecular level to execute the germination pathway and whether additional proteins are required remain unknown. Here, we sought to determine whether there were additional factors involved in degradation of the spore

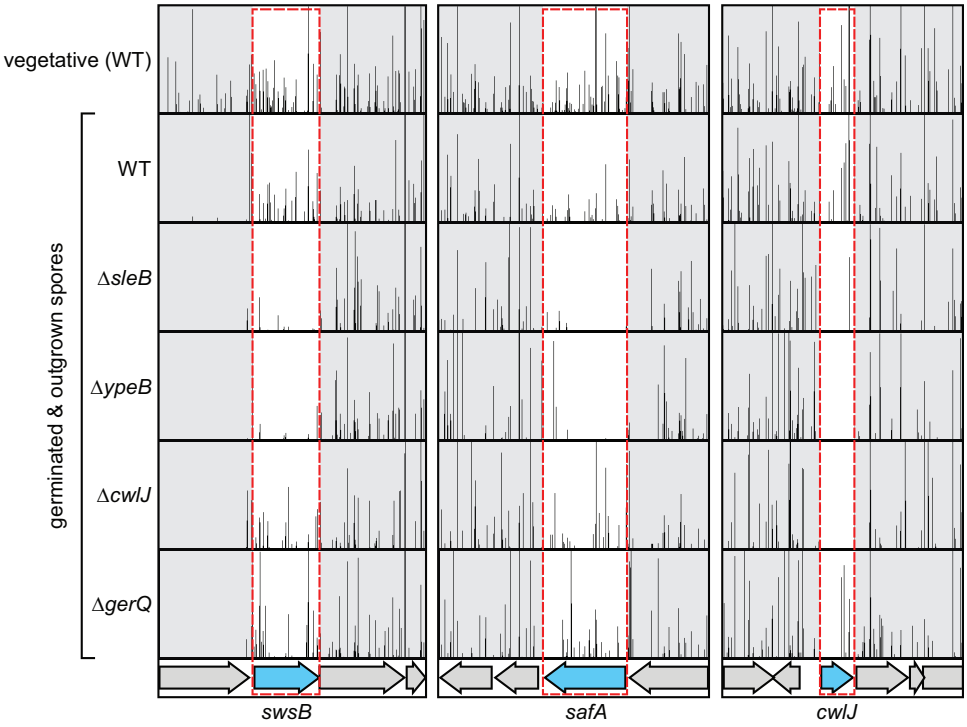

FIG 1 Transposon insertions in *swsB* and *safA* are underrepresented in germinated and outgrown spores lacking *sleB* or *ypeB*. Transposon insertion profiles of germinated and outgrown spores at three genomic locations were prepared. Transposon libraries generated in strains of the indicated genotype were sporulated by nutrient exhaustion for 30 h. Cultures were heat treated and then plated on LB agar. Colonies from germinated and outgrown spores ("germinated & outgrown spores") from each library were separately pooled, and transposon junctions were deep sequenced and mapped to a reference genome. At the onset of starvation, a sample of wild-type (WT) cells was collected ("vegetative"), and the transposon insertions were mapped. The regions containing the *swsB*, *safA*, and *cwlJ* genes (blue) are shown. The height of each line corresponds to the number of transposon insertions mapped to that locus, with the height of each box set at 250 reads.

cortex. We describe the identification and characterization of YlxY (SwsB) and its role in the CwlJ-dependent germination pathway.

RESULTS

A genetic screen for factors involved in cortex degradation. To investigate whether additional factors are required for the activity of SleB and CwlJ, we took advantage of the functional redundancy of the two cortex lytic enzymes and performed synthetic germination defect screens using transposon sequencing (Tn-seq) (34). We reasoned that transposon insertions in genes that were necessary for the proper functioning of CwlJ would impair germination in spores lacking SleB. These insertions would therefore be underrepresented in a transposon library generated in a Δ*sleB* mutant after sporulation, germination, outgrowth, and colony formation. Similarly, transposon insertions in genes required for SleB function would be underrepresented after germination and outgrowth of Δ*cwlJ* mutant spores. We generated transposon libraries in the *B. subtilis* 168 genome (here referred to as "wild type"), as well as in isogenic strains that were deficient in SleB-mediated (Δ*sleB* or Δ*ypeB*) or CwlJ-mediated (Δ*cwlJ* or Δ*gerQ*) cortex degradation. The libraries were sporulated by nutrient exhaustion in liquid sporulation medium for 30 h. The cultures were heat treated to kill vegetative cells and defective spores and then plated on nutrient-rich medium to trigger spore germination, outgrowth, and colony formation. A total of >500,000 colonies from each library were separately pooled, and the transposon insertion sites were mapped by deep sequencing. The insertion profiles were compared to each other and to the profile of the wild-type transposon library at the onset of starvation (Fig. 1; see Fig. S1 in the supplemental material).

Consistent with the idea that SleB and CwlJ are functionally redundant, transposon insertions were readily detected in *sleB*, *ypeB*, *cwlJ*, and *gerQ* in the wild-type library before and after sporulation, germination, and outgrowth (Fig. 1 and Fig. S1). Furthermore, and in validation of these screens, transposon insertions in *gerQ* and *cwlJ* were virtually undetectable in the strains lacking SleB or YpeB. Likewise, insertions in *sleB* and *ypeB* were absent in strains that lacked CwlJ or GerQ (Fig. 1 and Fig. S1). Consistent with the idea that GerQ and CwlJ are in the same pathway, insertions in *gerQ* were tolerated in the strain lacking CwlJ. Similarly, insertions in *ypeB* were tolerated in the strain lacking SleB (Fig. 1 and Fig. S1).

In further validation of these screens, transposon insertions in *cotE* were underrepresented in cells lacking SleB or YpeB (Fig. S1). These findings are consistent with previous studies showing that CotE is required for proper assembly of the spore coat and thus for proper localization and retention of CwlJ (28). Importantly, the *cotE* locus readily tolerated transposon insertions in outgrown spores lacking CwlJ and GerQ, confirming that CotE plays no role in the SleB germination pathway.

Our Tn-seq screen identified two additional genes, *ylxY* and *safA*. SafA has been previously implicated in the localization of CwlJ (35), but no functional studies have been reported. YlxY has not been previously linked to CwlJ function. Insertions in *ylxY* and *safA* were underrepresented in outgrown spores lacking SleB and YpeB but were readily tolerated in those lacking CwlJ and GerQ (Fig. 1). Thus, YlxY and SafA are potential new members of the CwlJ cortex degradation pathway. Based on the analysis described below, we renamed the *ylxY* gene *swsB* (pronounced "swiss B") for synthetic with sleB. In contrast, other than *sleB* and *ypeB*, there were no genes in which transposon insertions were specifically underrepresented in the absence of CwlJ and GerQ. Although we cannot rule out the possibility that functionally redundant or sporulation-essential factors affect SleB activity, these findings suggest that YpeB is the central regulator of SleB function (see Discussion).

SwsB is predicted to be a secreted protein with homology to polysaccharide deacetylases. It is a member of the carbohydrate esterase family 4 (CE4), a broadly conserved family of enzymes that spans all three domains of life and is responsible for deacetylating a wide variety of polysaccharides, including bacterial peptidoglycan (Fig. S2) (36). SwsB was previously reported to be a conserved protein among endospore-forming bacteria, suggesting that it functions in sporulation (37). Furthermore, the *swsB* promoter was found to be transcribed by the mother cell transcription factor SigE (38). However, there has been no phenotype identified for the Δ*swsB* mutant, and no function has been ascribed to SwsB to date.

To validate whether *swsB* is a member of the CwlJ pathway, we analyzed spore viability of a *swsB* deletion mutant in the wild type and in cells lacking SleB or CwlJ. The strains were sporulated by nutrient exhaustion, followed by heat treatment and plating on nonselective medium. Using this assay, the wild-type heat-resistant spore viability was $\sim 3.8 \times 10^8$ CFU per milliliter, whereas the Δ*sleB* Δ*cwlJ* double mutant was reduced $>10^7$-fold to ~25 CFU/ml (Fig. 2A). The Δ*cwlJ* or Δ*swsB* single mutants were not significantly affected in spore viability relative to the wild type, while spores lacking SleB were reduced in viability to 66% of wild-type levels. Consistent with the Tn-seq results, we observed a synergistic defect in the Δ*swsB* Δ*sleB* double mutant with spore viability reduced to 4% of wild-type levels (Fig. 2A). Finally, spore viability of the Δ*swsB* Δ*cwlJ* double mutant was similar to the wild type. These results suggest that SwsB specifically functions in the CwlJ pathway.

SafA is a morphogenetic protein that is required for proper assembly and maintenance of the spore coat (39). To establish whether SafA is a member of the CwlJ pathway and, like CotE, potentially involved in CwlJ retention in spores, we analyzed spore viability of a Δ*safA* mutant in a wild-type background and in cells lacking SleB and CwlJ. We then compared these to strains in which *cotE* or *gerQ* were disrupted alone or in combination with mutations in *sleB* or *cwlJ*. As expected, cells lacking SafA or GerQ, either alone or in combination with Δ*cwlJ*, had no significant decrease in spore viability. Mutants lacking CotE had a modest reduction in spore viability (45% that of the wild

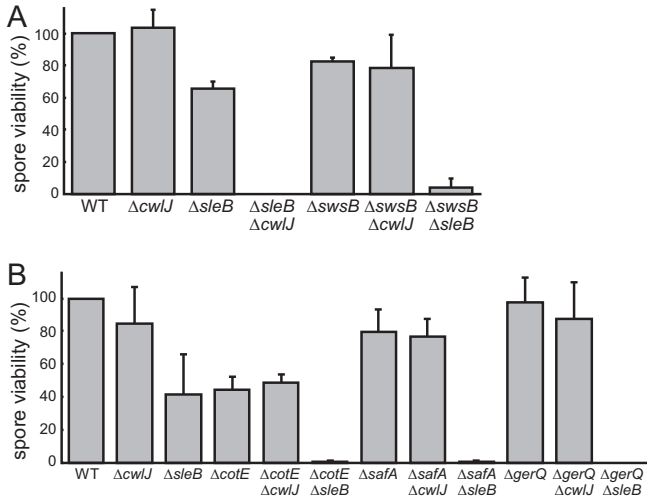

FIG 2 Validation of hits from the Tn-seq screen. Spore viability of mutant spores relative to the wild type. Cells of the indicated genotype were sporulated by nutrient exhaustion and heat treated, and serial dilutions were plated on LB agar to assess heat-resistant CFU. The wild-type (WT) spore viability (~3.8×10^8 CFU/ml) was set to 100%. (A) Spore viability of the Δ*swsB* mutant alone and in combination with Δ*sleB* and Δ*cwlJ*. (B) Spore viability of Δ*cotE*, Δ*safA*, and Δ*gerQ* coat mutants alone and in combination with Δ*sleB* and Δ*cwlJ*. Error bars indicate the standard deviations ($n = 3$).

type), and disrupting *cwlJ* in Δ*cotE* cells did not further reduce spore viability (Fig. 2B). Importantly, disruption of *cotE*, *safA*, or *gerQ* in Δ*sleB* cells led to a dramatic reduction in spore viability. Specifically, Δ*gerQ* Δ*sleB* spores phenocopied Δ*sleB* Δ*cwlJ* spores, with fewer than ten viable spores per milliliter of culture, while Δ*cotE* Δ*sleB* and Δ*safA* Δ*sleB* spores were decreased in spore viability to 0.4 and 0.3% of the wild type, respectively. This synergistic decrease validates our screen and, consistent with previous localization studies (35), places SafA in the CwlJ pathway.

SwsB is required for CwlJ-dependent germination. The experiments described above assayed for multiple aspects of spore viability and therefore could not distinguish between potential defects in spore formation, heat resistance, germination, or outgrowth. However, because SleB and CwlJ are thought to act exclusively during spore germination, the synergistic phenotype of the Δ*swsB* Δ*sleB* double mutant suggested that SwsB is similarly required for germination. To investigate this, we analyzed spores using phase-contrast microscopy. Dormant spores have reduced water content in their cores, resulting in a refractive index that makes them appear bright when visualized by phase-contrast microscopy. Germinating spores transition from phase bright to phase gray upon release of Ca^{2+}-DPA and uptake of water. Degradation of the cortex by SleB and CwlJ removes the physical constraints on core hydration and allows the spore to swell and become phase dark. Hydration restores metabolic activity and macromolecular synthesis leading to outgrowth. Accordingly, we used these cytological changes to assess spore germination and outgrowth.

Phase-bright spores were purified from heat-treated, sporulating cultures using density gradient centrifugation. They were then incubated in nutrient-rich medium (lysogeny broth-Lennox [LB]) at 37°C with agitation. Samples were then analyzed by phase-contrast microscopy before and at 30-min intervals after exposure to nutrients. As seen in Fig. 3, >99% of all spore samples were phase-bright prior to the addition of LB. After 30 min of incubation in LB, 100% of wild-type spores were phase-dark and swollen, indicating the successful completion of germination. By 90 min, virtually all the wild-type spores had initiated outgrowth. In contrast, <0.1% of Δ*sleB* Δ*cwlJ* spores were phase dark after 90 min in LB. Virtually all were phase gray in appearance, indicating that they had initiated germination and released Ca^{2+}-DPA but were unable to degrade the spore cortex (Fig. 3). Spores lacking CwlJ were delayed by ~30 min in the transition to phase-dark, but most had initiated outgrowth by 90 min. Approxi-

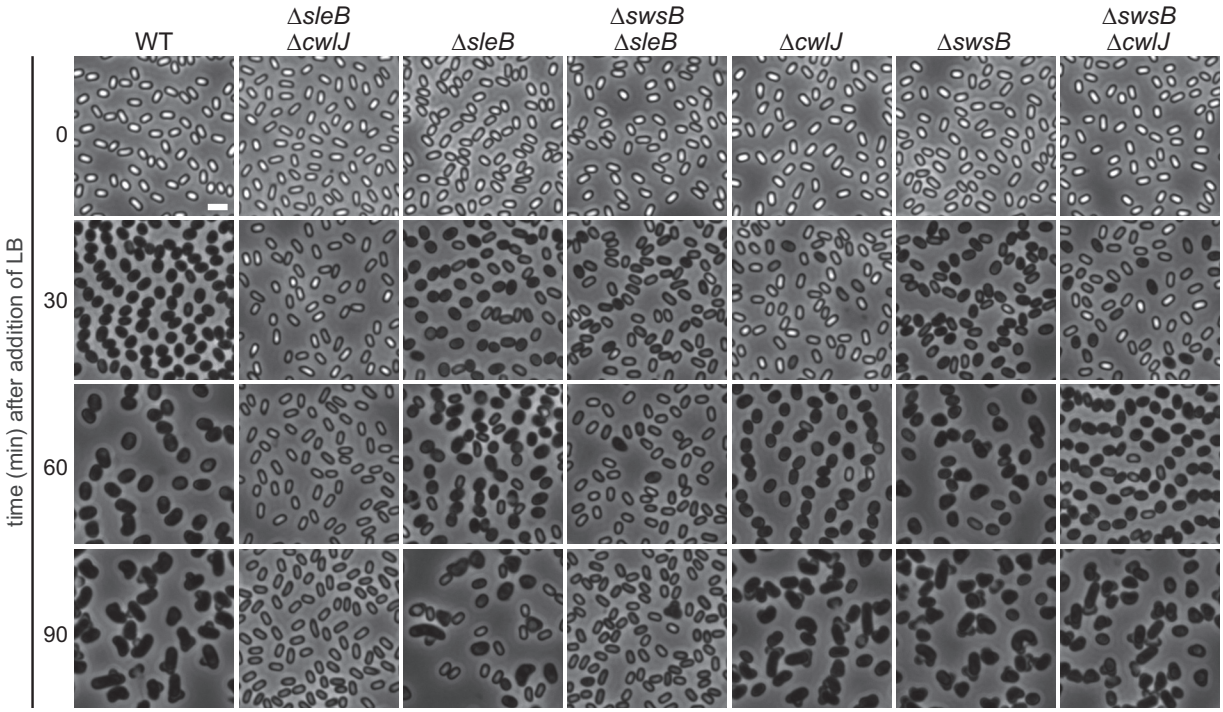

FIG 3 SwsB is required for germination in spores lacking SleB. Phase-contrast microscopy of spores germinating in LB was performed. Spores of the indicated genotype were purified by density gradient centrifugation and imaged before and at 30-min intervals after resuspension in LB at 37°C with agitation. Experiments were performed in biological triplicate, with representative images shown. For each sample, >1,000 spores were scored at the 90-min time point. The scale bar (2 μm) applies to all images in the paper.

mately half of the Δ*sleB* spores transitioned from phase bright to phase dark 30 min after LB addition with the remainder becoming phase gray. Consistent with the spore viability assay, 59% of Δ*sleB* single mutant spores had initiated outgrowth by 90 min. Germination and outgrowth in the absence of SwsB were similar to the wild type with a modest lag in germination for a subset of spores. In support of the idea that SwsB functions in CwlJ-dependent germination, virtually all the Δ*swsB* Δ*sleB* double mutant spores transitioned to phase gray by 30 min, but only 4.4% had outgrown by 90 min (Fig. 3). Importantly, the Δ*swsB* Δ*cwlJ* double mutant largely phenocopied the Δ*cwlJ* single mutant, consistent with the idea that these factors are in the same pathway. Similar results were obtained using purified spores from non-heat-treated sporulating cultures, indicating that the thermostability of CwlJ is not influenced by SwsB. Altogether, these data indicate that the defects in spore viability observed in the plating assay are fully accounted for by defects in spore germination.

To further investigate the role of SwsB in germination, we performed similar experiments using the germinant L-alanine. L-alanine triggers exit from dormancy but does not provide sufficient nutrients for outgrowth, so germinating spores remain stalled at the swollen phase-dark stage. Similar to our LB experiments, >90% of the wild-type, Δ*cwlJ*, Δ*swsB*, and Δ*swsB* Δ*cwlJ* spores and <0.1% of the Δ*sleB* Δ*cwlJ* spores germinated within 90 min of addition of L-alanine (Fig. 4). Importantly, 41% of Δ*sleB* spores germinated after 90 min, and this was reduced to 4% in the Δ*swsB* Δ*sleB* double mutant. These data provide additional evidence that SwsB functions in the CwlJ-dependent germination pathway.

Finally, to confirm that SwsB has an effect exclusively on CwlJ-dependent cortex degradation, we took advantage of the fact that CwlJ-dependent germination can be triggered by the addition of exogenous Ca^{2+}-DPA (40), which is thought to mimic its release from the spore upon detection of nutrients. Spores were analyzed by phase-contrast microscopy before and at 30-min intervals after incubation with 60 mM Ca^{2+}-DPA at 22°C with agitation. By 120 min after the addition of Ca^{2+}-DPA, 63% of the

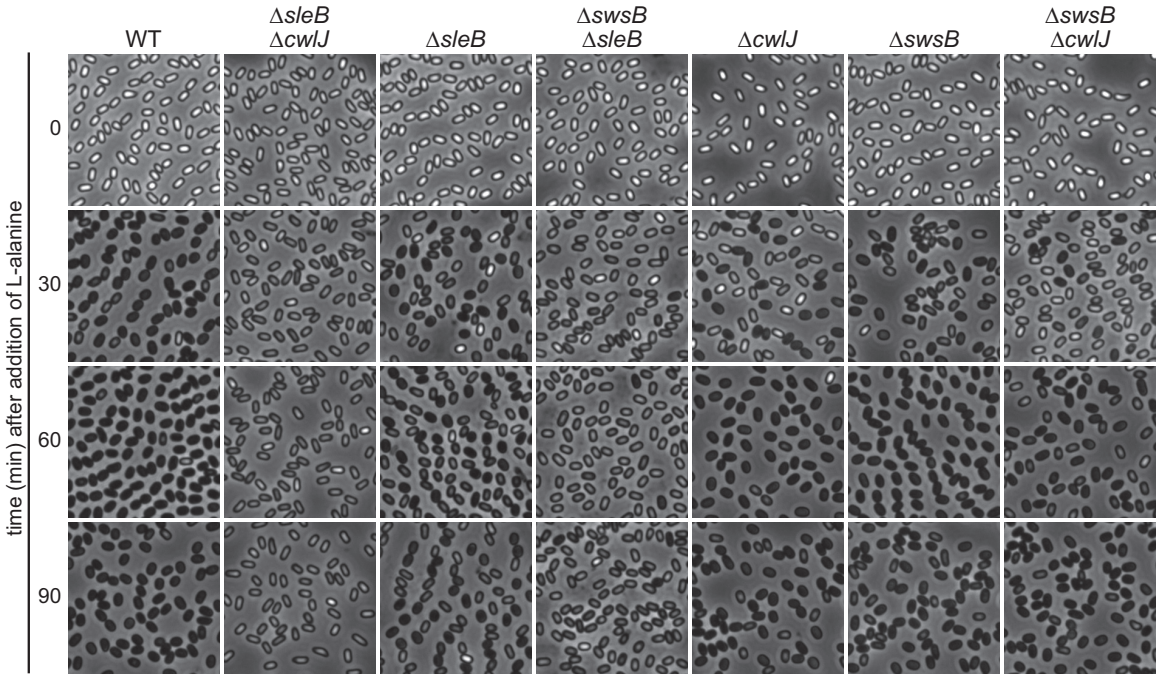

FIG 4 SwsB is required for L-alanine-mediated germination in spores lacking SleB. Phase-contrast microscopy of spores germinating in L-alanine was performed. Spores of the indicated genotype were purified by density gradient centrifugation and imaged before and at 30-min intervals after resuspension in 5 mM L-alanine at 37°C with agitation. Experiments were performed in biological triplicates, with representative images shown. For each sample, >1,000 spores were scored at the 90-min time point.

wild-type spores and 57% of the Δ*sleB* spores had undergone germination (Fig. S3). As anticipated, no germination was observed (<0.1%) in spores that lacked CwlJ (Δ*cwlJ*, Δ*cwlJ* Δ*sleB*, and Δ*swsB* Δ*cwlJ*), confirming that CwlJ is responsible for germination in the presence of exogenous Ca^{2+}-DPA. Consistent with the idea that SwsB functions in the CwlJ pathway, spores lacking SwsB had reduced germination at 4% that of the wild type. We note that the germination defect was as pronounced as the 4 to 5% germination observed in the Δ*swsB* Δ*sleB* double mutant in LB and L-alanine. This germination defect argues that SwsB specifically functions to promote CwlJ-dependent cortex degradation.

Conserved residues in SwsB are required for germination. CE4 deacetylases have several highly conserved motifs known to be involved in catalysis. SwsB contains most of these but appears to be missing a conserved charge pair that constitute the essential catalytic base of other CE4 enzymes (41, 42) (Fig. S2). To investigate whether other conserved motifs are important for SwsB function, we focused on a catalytic charge pair consisting of an aspartic acid at position 256 (D256) and a histidine at position 282 (H282). We generated amino acid substitutions in the context of a functional SwsB-hexahistidine fusion (SwsB-His) and introduced them at an ectopic chromosomal locus in the Δ*swsB* Δ*sleB* double mutant. We then assayed spore viability after heat treatment to assess germination efficiency. As described above, Δ*sleB* spores exhibited viability at 55% that of the wild type, while Δ*swsB* spores exhibited 100% viability (Fig. 5A). The Δ*swsB* Δ*sleB* double mutant spores had a synergistic defect with 6.9% viability compared to the wild type. Importantly, the ectopic *swsB-His* allele was able to fully complement spore viability in the Δ*swsB* Δ*sleB* double mutant, with spore viability reaching 62%. However, *swsB-His* fusions encoding either H282 mutated to alanine (H282A) or D256 mutated to alanine or asparagine (D256A, D256N) failed to complement the *swsB* deletion, with spore viability of the Δ*swsB* Δ*sleB* mutant remaining at 4.6 to 7.2% of the wild type. None of these mutations affected protein stability of SwsB in sporulating cells, as assayed by immunoblot analysis (Fig. 5B). These data indicate that H282 and D256 are required for SwsB function in spore germination and raised the possibility that SwsB is a polysaccharide deacetylase.

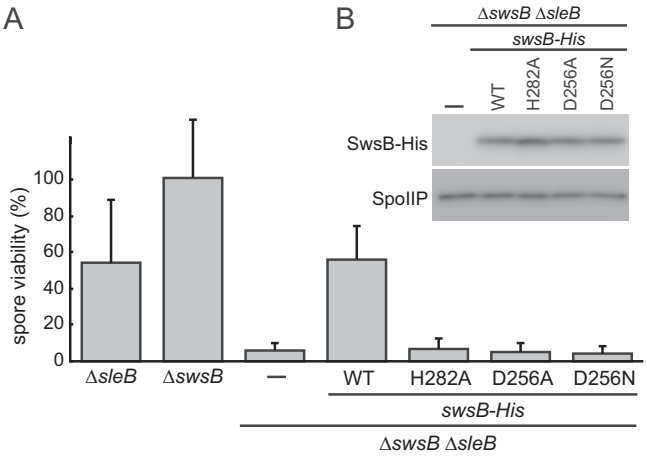

FIG 5 Conserved residues in SwsB are required for function. Complementation of Δ*swsB* Δ*sleB* with ectopically expressed *swsB* alleles. (A) Spore viability of the Δ*swsB* Δ*sleB* double mutant harboring wild-type *swsB*, a tagged version of SwsB containing a C-terminal hexahistidine tag (product of *swsB-His*), or products of *swsB-His* with various mutated residues (H282A, D256A, and D256N). Cells of the indicated genotype were sporulated by nutrient exhaustion, heat treated, and plated on LB to assess heat-resistant CFU. Wild-type spore viability (~3.8×10^8 CFU/ml) was set to 100%. (B) Immunoblots of SwsB-His variants. The indicated strains were sporulated by resuspension, and samples were collected at h 3 (T3). Lysates were subjected to SDS-PAGE, followed by immunoblot analysis, to detect the presence of the hexahistidine tag (SwsB-His) or a sporulation-specific loading control (SpoIIP). Immunoblots are representatives of two biological replicates.

SwsB does not detectably modify spore peptidoglycan. Because SwsB requires a conserved deacetylase motif and plays a role in promoting CwlJ activity, we hypothesized that SwsB deacetylates cortex peptidoglycan, thereby creating CwlJ's preferred substrate. To investigate this model, we performed muropeptide analysis on cortex peptidoglycan from wild-type and Δ*swsB* spores. In addition, we generated spores from a strain in which *swsB* was expressed from strong mother cell (P_{spoIID}) and forespore (P_{sspB}) promoters. We refer to this overexpression strain as $swsB^{OE}$. Both promoter fusions could separately complement the Δ*swsB* mutant, as measured by the restoration of spore viability to the Δ*swsB* Δ*sleB* mutant (Fig. S4). The restoration of spore viability suggests that SwsB is likely to be expressed in the $swsB^{OE}$ strain at least 2-fold above the wild-type levels. All three strains were first sporulated by nutrient exhaustion. Spores were then purified from vegetative cells using lysozyme and SDS. The purified spores were then decoated by chemical and enzymatic treatment, and spore peptidoglycan was isolated. Insoluble peptidoglycan was digested with muramidase to generate soluble fragments that were subjected to ultraperformance liquid chromatography (UPLC), followed by mass spectrometry (MS).

Figure 6 shows the UV absorbance chromatogram of the UPLC-analyzed samples. The chromatograms from all three samples are highly similar, with no species dramatically under-represented in the Δ*swsB* sample or overrepresented in the $swsB^{OE}$ sample. Further analysis of the total ion current chromatogram and the corresponding mass spectra showed very little deacetylated peptidoglycan. As seen in Fig. 6, Fig. S5 and S6, and Table S1, peaks 5 and 16 correspond to the only muropeptide fragments in which a deacetylated residue was detected. In both, a MurNAc residue was the deacetylated species (Fig. S7), and these remained unchanged in our mutants. Thus, SwsB has no measurable effect on the acetylation status of spore peptidoglycan.

Investigating other functions for SwsB. The lack of detectable changes in deacetylated PG in Δ*swsB* spores suggested that SwsB influences CwlJ by some other mechanism. We investigated three possibilities: (i) SwsB is required for CwlJ retention in spores, (ii) SwsB is required for the accumulation of Ca^{2+}-DPA in the spore core, and (iii) SwsB functions as a cofactor for CwlJ activity during germination. To test whether SwsB influences CwlJ accumulation and/or retention in spores, we constructed a

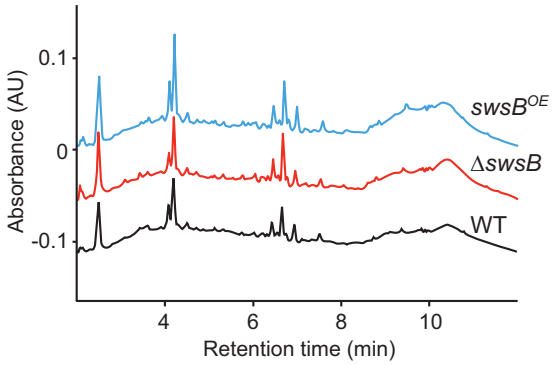

FIG 6 Muropeptide analysis of spore peptidoglycan. UPLC chromatograms of muropeptide fragments derived from purified spores from wild-type (WT), Δ*swsB*, and SwsB overexpression (*swsB*^{OE}) strains. The spores were decoated, and the cell wall peptidoglycan layers were solubilized by digestion with muramidase. Fragments were separated by UPLC and monitored by UV absorbance at 204 nm measured in arbitrary units. Chromatograms have been arbitrarily offset and overlaid for illustrative purposes. Three biological replicates were performed for each sample; representative chromatograms are shown. This analysis would likely have detected differences between strains of ≥10%.

C-terminally tagged version of CwlJ (CwlJ-His) to monitor its level in purified spores. The *cwlJ-His* allele was able to partially complement Δ*cwlJ*, as measured by its ability to restore spore viability to a Δ*sleB* Δ*cwlJ* mutant from fewer than 10 viable spores per milliliter to 4.4×10^6 spores/ml, or ~1% of the wild type (Fig. S8). We compared CwlJ-His levels in wild-type and Δ*swsB* spores by immunoblotting (Fig. 7A). As a control, we examined the CwlJ-His levels in Δ*gerQ* and Δ*cotE* mutant spores, because both are required for CwlJ accumulation (28, 32). Finally, we also monitored CwlJ levels in Δ*safA* spores to test whether this new pathway member impacts CwlJ accumulation. As anticipated, the levels of CwlJ-His were reduced in Δ*gerQ* and Δ*cotE* spores. CwlJ-His levels were also lower in the Δ*safA* mutant, providing an explanation for the synthetic germination defect between Δ*safA* and Δ*sleB* mutants. However, the level of CwlJ-His in Δ*swsB* spores was similar to that for the wild type, ruling out a role for SwsB in CwlJ accumulation.

Next, we tested whether Ca^{2+}-DPA accumulation was impaired in Δ*swsB* spores. Because this metabolite is required for CwlJ activity, a reduction in its accumulation in cells lacking SwsB could account for the mutant phenotype. Purified spores were collected and boiled to release DPA, which was then measured by fluorescence using $TbCl_2$ (43, 44). Wild-type spores and spores lacking the DPA synthase (SpoVFA) or the DPA import machinery (SpoVA) served as our positive and negative controls. In spores lacking SwsB, SleB, or CwlJ, alone or in all double mutant combinations, the DPA levels were similar to those for the wild type (Fig. 7C). This ruled out a role for SwsB in DPA accumulation.

Finally, to explore whether SwsB functions as a cofactor with CwlJ during germination, we investigated whether SwsB is present in spores or present only during sporulation. Previous studies did not detect SwsB in the coat of dormant spores, arguing that SwsB does not act with CwlJ during germination (45–49). To test this more directly, we compared SwsB-His levels in dormant spores to levels in cells 3 h after the initiation of sporulation. As can be seen in Fig. 7B, SwsB was readily detectable in sporulating cells but undetectable in dormant spores. CwlJ-His and SigA served as controls for spore-associated proteins and for our anti-His antibody. Although we cannot rule out the possibility that the His tag on SwsB is degraded in dormant spores, these data argue that SwsB is not present in spores and therefore is unlikely to act as a CwlJ cofactor during germination. Collectively, these results indicate that SwsB does not play a role in the localization of CwlJ to spores nor in DPA accumulation in the core. The data further suggest that SwsB acts during spore formation and only indirectly impacts CwlJ activity during germination.

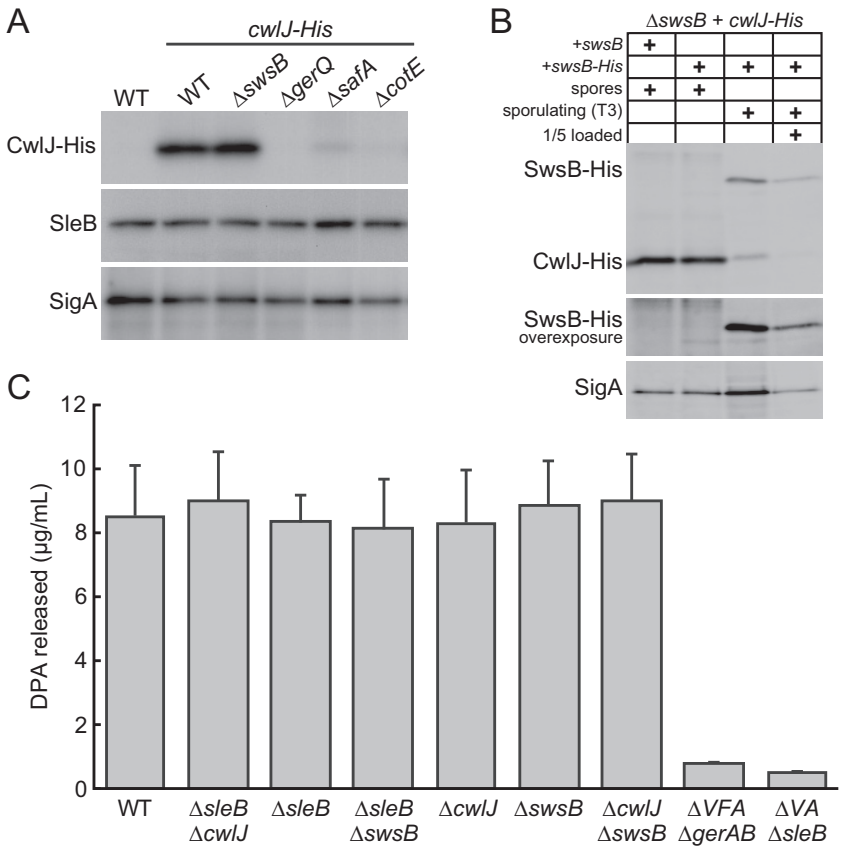

FIG 7 Analysis of potential functions for SwsB in spore biology. (A) SwsB is not required for CwlJ accumulation in spores. Histodenz-purified spores were lysed by physical disruption and subjected to SDS-PAGE, followed by immunoblot analysis, to detect hexahistidine-tagged CwlJ (CwlJ-His). SleB and SigA were analyzed to control for loading. (B) SwsB-His is undetectable in dormant spores. Spores harboring hexahistidine-tagged versions of CwlJ (CwlJ-His) and SwsB (SwsB-His) were lysed by physical disruption and normalized based on total protein content. Samples were then subjected to SDS-PAGE, followed by immunoblot analysis with anti-His antibodies, to detect CwlJ-His and SwsB-His. SigA was analyzed to control for loading. SwsB-His was undetectable even upon overexposure of the immunoblot. To control for the ability to detect SwsB-His, sporulating cells at h 3 (T3) were analyzed on the same immunoblot. SwsB-His was readily detectable during sporulation even when one-fifth of the amount of lysate was loaded. (C) Spores lacking SwsB accumulate wild-type levels of DPA. Histodenz-purified spores of the indicated strains were boiled to release DPA. DPA was then measured by fluorescence using $TbCl_3$. Error bars show standard deviations ($n = 3$). Immunoblots are representatives of two biological replicates.

DISCUSSION

Our synthetic germination defect screen identified two new factors that impact CwlJ activity. CwlJ is known to require the coat proteins CotE and GerQ for accumulation in dormant spores, and here we show that another coat protein, SafA, is similarly required for CwlJ accumulation. Based on the known localization pathway of coat proteins (19), we propose that SafA and CotE are incorporated into the spore coat at an early stage of coat assembly, and these proteins then function in the recruitment of GerQ and in turn CwlJ. The second new factor, SwsB (formerly YlxY), is produced in the mother cell during sporulation (38) and is likely secreted into the intermembrane space (50, 51). Our data strongly suggest that SwsB is required to promote CwlJ activity during germination yet does not affect CwlJ accumulation in the dormant spore nor the amount of DPA present in the core. Furthermore, SwsB does not appear to be present in dormant spores and therefore likely acts prior to spore maturation. Given that SwsB is homologous to polysaccharide deacetylases and has conserved catalytic residues required for its function, the simplest interpretation of these data is that SwsB directly or indirectly modifies the spore cortex, thereby generating a substrate that CwlJ can efficiently

cleave during germination. However, our analysis of spore PG failed to detect any substantial changes in cortex structure in the absence of SwsB or in the presence of increased expression of the protein.

We are therefore left to speculate on SwsB function. We favor a model in which SwsB modifies spore cortex, but the extent of modification is too modest to be detected by bulk muropeptide analysis. This subtle modification could then have a profound effect on CwlJ, whose activity may be acutely sensitive to SwsB-modified cortex. One possible reason that SwsB modification is difficult to detect is that SwsB may be responsible only for deacetylating a sublayer of cortex. Lending credence to this idea, previous studies have shown that the cortex is not homogenous but rather has gradients of modifications across its span (14). In addition, it is notable that the main deacetylase involved in muramic delta-lactam formation, PdaA, is produced in the forespore under SigG control (52). An attractive model is one which supposes that PdaA is responsible for making the bulk of the muramic delta-lactam but SwsB, produced by the mother cell, has access to and is responsible for synthesizing the outermost layer of muramic delta-lactam in the developing cortex. It is this outermost layer which would then be the first substrate encountered by CwlJ.

We can also imagine a model in which SwsB binds the spore cortex but does not modify it; rather, SwsB binding occludes or activates other enzymes whose activity alters CwlJ cleavage. Much like in the first model, this induced modification could then escape our detection by being too modest or by changing only one sublayer of cortex. In support of this model is the fact that SwsB is missing several highly conserved residues normally involved in catalysis. In addition, our analysis of purified recombinant SwsB using two different deacetylase assays failed to identify any activity *in vitro*. This is despite deacetylase activity being readily detectable using the *Bacillus cereus* deacetylase Bc1960 (42) purified under identical conditions.

Finally, a third possibility is that other polysaccharides are deposited in the spore and SwsB acts on them. These polysaccharides, without the modifications generated by SwsB, would impair CwlJ activity. Indeed, bioinformatic analyses have found several putative glycosyltransferases that are predicted to be under SigK and SigE control (53). Some of these are responsible for glycosylating proteins in the spore crust, while others are of unknown function. Furthermore, previous work in our laboratory has discovered a putative flippase that could potentially transport an uncharacterized lipid-linked precursor to the intermembrane space of the developing spore (4). This precursor could be used to synthesize an alternative polysaccharide, which itself may have an effect on CwlJ.

SwsB is broadly conserved and likely functions similarly in other spore formers, although we note that most organisms that have CwlJ lack a discernible SwsB homolog, implying that CwlJ does not always require SwsB (see Fig. S9 in the supplemental material). Our bioinformatics analysis found that SwsB-like proteins, as defined as CE4 family enzymes that lack a catalytic basic charge-pair, can be found throughout the *Bacilli* and *Clostridia* classes (Fig. S2B; Data Set S1). What would be the evolutionary driving force to maintain *swsB* in these disparate genomes? We suspect that SwsB evolved to protect the cortex from degradative enzymes and that CwlJ specificity was altered to retain activity on this material. However, of the 180 organisms with a SwsB-like protein, only 106 have CwlJ. It is therefore possible that in the remaining 74 organisms SleB has evolved to retain activity on SwsB-modified cortex instead of CwlJ, but the role of SwsB in these organisms awaits further testing.

Finally, our genetic screen failed to identify additional factors other than YpeB that specifically function in the SleB germination pathway. These results cannot rule out the existence of redundant factors or sporulation-essential proteins that control SleB activity during germination. However, our findings raise the possibility that YpeB is the only factor involved in the direct regulation of SleB. This leads us to speculate that the SleB-YpeB pathway is itself directly regulated and activated by known factors like SpoVA and GerA family receptors required for germination.

MATERIALS AND METHODS

General methods. All *B. subtilis* strains were derived from the auxotrophic (*trpC2*) strain 168 (54). To obtain spores, sporulation was induced by nutrient exhaustion in liquid medium. Cells were grown in supplemented Difco sporulation medium (DSM) at 37°C with agitation for 24 to 30 h. To obtain synchronous sporulating cultures, sporulation was induced by resuspension according to the method described by Sterlini and Mandelstam (55). Spore viability was determined by comparing the total number of heat-resistant (80°C for 20 min) CFU as a percentage of the wild-type heat-resistant CFU. Deletion mutants were derived from the *Bacillus* knockout (BKE) collection (56) or were generated by isothermal assembly of PCR products (57), followed by direct transformation into *B. subtilis*. All BKE mutants were backcrossed twice in *B. subtilis* 168 before assaying and prior to antibiotic cassette removal. Antibiotic cassette removal was performed using a temperature-sensitive plasmid that constitutively expresses Cre recombinase (58). All strains were constructed using a one-step competence method. Tables of strains, plasmids, and primers used in this study can be found in supplemental material.

Transposon insertion sequencing. Tn-seq was performed as described previously (4). Briefly, DNA from a Magellan6x transposon library was transformed into competent *B. subtilis* cells of various genotypes. More than 500,000 transformants were pooled, aliquoted, and frozen at −80 °C. An aliquot was thawed, washed in DSM, and diluted into 50 ml of supplemented DSM at an optical density at 600 nm (OD_{600}) of 0.05. Cells were sporulated via nutrient exhaustion in liquid sporulation medium at 37°C for 30 h. Cultures were then incubated at 80°C for 20 min to select for heat-resistant spores and plated on LB agar. Over 500,000 colonies from each genotype were separately pooled. Genomic DNA was extracted and digested with MmeI. Adapters were ligated, and transposon-chromosome junctions were amplified using 16 PCR cycles. PCR products were gel purified and sequenced on the Illumina HiSeq platform using TruSeq reagents (Tufts University TUCF Genomics facility). Reads were mapped to the *B. subtilis* 168 genome (NCBI NC_00964.3), tallied at each TA site and subjected to Mann-Whitney U testing for statistically underrepresented genes. Visual inspection of transposon insertion profiles was performed with the Sanger Artemis genome browser and annotation tool (59).

Spore purification. A portion (10 ml) of overnight DSM culture was heat treated (80 °C for 20 min) and washed three times with sterile H_2O. The spore pellet was resuspended in 1 ml of 20% (wt/vol) Histodenz (Sigma) and incubated for 30 min on ice. This suspension was then gently pipetted on top of a two-step Histodenz gradient consisting of 2 ml of 40% (wt/vol) Histodenz layered on 6 ml of 50% (wt/vol) Histodenz. The gradient was centrifuged at 4,000 rpm for 90 min at 23°C, and the supernatant, which contained phase-dark spores, vegetative cells, and cell debris, was siphoned off. The pellet was washed three times with sterile H_2O. Pellets were either resuspended in 1 ml of H_2O and kept at 4°C for germination experiments or in 0.5 ml of phosphate-buffered saline (PBS) with protease inhibitors and kept on ice for protein extraction. All spore preparations were evaluated by phase-contrast microscopy and contained >99% phase bright spores.

Microscopy. To monitor spore germination and outgrowth, purified spores were concentrated and then resuspended in LB or L-alanine (5 mM), followed by incubation with agitation at 37°C. Alternatively, 60 mM Ca^{2+}-DPA was freshly mixed (equal volumes of 120 mM $CaCl_2$ and 120 mM DPA [Tris to pH 8.0]) and used to resuspend concentrated spores, which were then incubated with agitation at 22°C (60 mM Ca^{2+}-DPA formed a precipitate when incubated at higher temperatures or stored for longer periods). Aliquots were removed at the indicated time points.

Dormant and germinating spores were concentrated by centrifugation and then immobilized on pads made of 2% (wt/vol) agarose in PBS. Phase-contrast microscopy was performed using a Nikon TE2000 inverted microscope, Nikon Intensilight Metal Halide Illumination, a Photometrics CoolSNAP HQ2 monochrome charge-coupled device camera, and a Plan Apo 100×/1.4-numerical-aperture oil Ph3 DM objective. All exposure times were 200 ms. Image acquisition was performed using Nikon Elements Acquisition Software AR 3.2. Image analysis and processing were performed in Metamorph. Representative images are shown. For the quantifications reported here, >1,000 spores for each sample were scored for a phase-bright, phase-gray, phase-dark, or outgrown appearance at the final time point.

SDS-PAGE and immunoblotting. Protein was extracted from sporulating cells as previously described (60). Briefly, cells were sporulated by resuspension (55). At the indicated time point, 1 ml of cells was collected and stored at −80°C. The cells were thawed on ice, resuspended in 50 μl of lysis buffer (20 mM Tris [pH 7.5], 10 mM EDTA, 1 mg/ml lysozyme, 1 mM phenylmethylsulfonyl fluoride, 10 μg/ml DNase I [New England Biolabs], 100 μg/ml RNase A [New England Biolabs]), and incubated at 37°C for 10 min. Then, 50 μl of 2× Laemmli sample buffer with 10% (vol/vol) β-mercaptoethanol was added, and the samples were heated to 80°C for 5 min. Samples were normalized based on the OD_{600} at the time of harvest.

To obtain total protein extracts from dormant spores, Histodenz-purified spores were suspended in 0.5 ml of PBS with protease inhibitors, added to 2-ml tubes containing lysing matrix B (MP Biomedicals, Irvine, CA), and chilled on ice. Spores were then ruptured mechanically using FastPrep (MP Biomedicals) at 6.5 m/s for 1 min. Then, 0.5 ml of 2× Laemmli sample buffer with 10% (vol/vol) β-mercaptoethanol was immediately added, and the tubes were vortexed. Samples were then incubated at 80°C for 5 min and centrifuged at maximum speed for 10 min. The supernatants were collected, and the total protein was normalized using a noninterfering protein assay (G-Biosciences, St. Louis, MO).

All samples were separated by SDS-PAGE on 17.5% resolving gels, electroblotted onto Immobilon-P membranes (Millipore, Burlington, MA), and blocked in 5% nonfat milk in PBS with 0.5% Tween 20. Membranes were then probed with monoclonal anti-His (1:4,000; GenScript), polyclonal anti-SpoIIP (1:20,000) (61), polyclonal anti-SigA (1:10,000) (62), or polyclonal anti-SleB (1:5,000) (31) diluted in 3% bovine serum albumin in PBS with 0.05% Tween 20. Primary antibodies were detected using horseradish

peroxidase-conjugated anti-mouse or anti-rabbit antibodies (Bio-Rad) and detected with Western Lightning ECL reagent as described by the manufacturer.

Isolation of spore PG. Portions (50 ml) of overnight DSM cultures were collected, washed three times with water, and resuspended in 2 ml of TE buffer. Lysozyme was added to a final concentration of 1 mg/ml, and the samples were incubated at 37 °C with shaking for 1 h. Sodium dodecyl sulfate (SDS) was added to a final concentration of 2% (wt/vol), and the samples were incubated at 37°C with shaking for an additional 20 min. Spores were spun down and washed repeatedly with water until all traces of SDS were undetectable (six to eight washes). Pellets were resuspended in water, imaged by phase-contrast microscopy, and verified to consist of >99% phase-bright spores. The spores were then treated with decoating solution (50 mM Tris-HCl [pH 8.0], 8 M urea, 1% [wt/vol] SDS, 50 mM dithiothreitol) twice for 60 min at 37°C. Decoated spores were washed five times in Milli-Q H_2O to fully remove the SDS. The spores were then resuspended in 1 ml of 1 M HCl, followed by incubation for 6 min at 100°C, and then washed once with 1 ml of 1 M Tris-HCl (pH 8.0) and five times with 1 ml of Milli-Q H_2O. The samples were then resuspended in 0.9 ml of trypsin digestion solution (20 mM Tris-HCl [pH 8.0], 10 mM $CaCl_2$, 0.1 mg/ml trypsin [TRTPCK; Worthington]) and incubated overnight at 37°C with shaking. The following day, SDS was added to a final concentration of 1% (wt/vol), and the samples were incubated at 100°C for 15 min. The samples were again washed five times in 1 ml of Milli-Q H_2O. Sacculi were then resuspended in 100 μl of 12.5 mM $NaHPO_4$, to which 40 U of mutanolysin from *Streptomyces globisporus* (Sigma) was added. Samples were incubated overnight at 37°C with shaking. Then, 50 μl of 10 mg/ml $NaBH_4$ was added, and the samples were incubated for 30 min at room temperature. Samples were then acidified by adding H_3PO_4 dropwise until reaching a pH of ~4, as measured by pH indicator paper. Samples were then lyophilized and resuspended in small volumes of water in preparation for liquid chromatography-mass spectrometry.

Liquid chromatography-mass spectrometry. An Acquity UPLC H-Class system (Waters, Milford, MA) equipped with a Xevo G2-XS QTOF (Waters) was used for liquid chromatographic studies. Separation of analytes was performed on a Waters BEH C_{18} column (pore size, 1.7 μm; 150 mm by 2.1 mm [inner diameter]). The mobile phase was as follows: solvent A (0.1% formic acid in Milli-Q water) and solvent B (0.1% formic acid in acetonitrile). The gradient used was as described previously (63). Wavelength was set at 204 nm for recording the chromatographic data.

Mass spectrometry was performed on a Xevo G2-XS QTOF (Waters) under conditions previously described (63). Waters UNIFI software was used for data acquisition and analysis. Plausible structures of muropeptides were drawn based on their molecular mass and fragmentation pattern data analysis.

Measuring Ca^{2+}-DPA levels. Spores were purified via Histodenz gradient and resuspended to an OD_{600} of 1 in water. Spore suspensions were then incubated at 100°C for 30 min to release Ca^{2+}-DPA. Suspensions were centrifuged, and supernatants were added to $TbCl_3$ at a final concentration of 25 mM (43, 44). Fluorescence was measured at 545 nm with excitation set at 272 nm. Three biological triplicates were performed, with each sample analyzed in technical triplicate and compared to a standard curve to determine DPA concentration.

SUPPLEMENTAL MATERIAL

Supplemental material is available online only.

SUPPLEMENTAL FILE 1, PDF file, 6.2 MB.

SUPPLEMENTAL FILE 2, XLSX file, 0.03 MB.

ACKNOWLEDGMENTS

We thank all members of the Bernhardt-Rudner supergroup past and present for helpful advice, discussions, and encouragement. We thank Paula Montero Llopis and the HMS Microscopy Resources on the North Quad (MicRoN) core at Harvard Medical School for advice on microscopy, Michael Welsh for advice on mass spectrometry, Hui Pan and Jonathan Dreyfuss at the Joslin Diabetes Center Bioinformatics and Biostatics core for bioinformatics consultation, and David Popham for helpful discussions.

Support for this work comes from the National Institute of Health (NIH) grant GM127399, DARPA HR001117S0029, and an HMS Dean's Innovation Award (D.Z.R.). J.D.A. was funded in part by NIH grant F32GM130003. Research in the Cava lab is supported by MIMS, the Knut and Alice Wallenberg Foundation (KAW), the Swedish Research Council, and the Kempe Foundation.

REFERENCES

1. Tan IS, Ramamurthi KS. 2014. Spore formation in *Bacillus subtilis*. Environ Microbiol Rep 6:212–225. https://doi.org/10.1111/1758-2229.12130.
2. Higgins D, Dworkin J. 2012. Recent progress in *Bacillus subtilis* sporulation. FEMS Microbiol Rev 36:131–148. https://doi.org/10.1111/j.1574-6976.2011.00310.x.
3. Ulrich N, Nagler K, Laue M, Cockell CS, Setlow P, Moeller R. 2018. Experimental studies addressing the longevity of *Bacillus subtilis* spores: the first data from a 500-year experiment. PLoS One 13:e0208425. https://doi.org/10.1371/journal.pone.0208425.
4. Meeske AJ, Rodrigues CDA, Brady J, Lim HC, Bernhardt TG, Rudner DZ. 2016. High-throughput genetic screens identify a large and diverse collection of new sporulation genes in *Bacillus subtilis*. PLoS Biol 14:e1002341. https://doi.org/10.1371/journal.pbio.1002341.
5. Stragier P, Losick R. 1996. Molecular genetics of sporulation in *Bacillus*

subtilis. Annu Rev Genet 30:297–241. https://doi.org/10.1146/annurev.genet.30.1.297.
6. Setlow P. 2014. Germination of spores of *Bacillus* species: what we know and do not know. J Bacteriol 196:1297–1305. https://doi.org/10.1128/JB.01455-13.
7. Moir A, Cooper G. 2015. Spore germination. Microbiol Spectr 3(6):TBS-0014-2012. https://doi.org/10.1128/microbiolspec.TBS-0014-2012.
8. Setlow P, Wang S, Li YQ. 2017. Germination of spores of the orders *Bacillales* and *Clostridiales*. Annu Rev Microbiol 71:459–477. https://doi.org/10.1146/annurev-micro-090816-093558.
9. Setlow B, Atluri S, Kitchel R, Koziol-Dube K, Setlow P. 2006. Role of dipicolinic acid in resistance and stability of spores of *Bacillus subtilis* with or without DNA-protective alpha/beta-type small acid-soluble proteins. J Bacteriol 188:3740–3747. https://doi.org/10.1128/JB.00212-06.
10. Magge A, Granger AC, Wahome PG, Setlow B, Vepachedu VR, Loshon CA, Peng L, Chen D, Li YQ, Setlow P. 2008. Role of dipicolinic acid in the germination, stability, and viability of spores of *Bacillus subtilis*. J Bacteriol 190:4798–4807. https://doi.org/10.1128/JB.00477-08.
11. Setlow P. 2006. Spores of *Bacillus subtilis*: their resistance to and killing by radiation, heat and chemicals. J Appl Microbiol 101:514–525. https://doi.org/10.1111/j.1365-2672.2005.02736.x.
12. Warth AD, Ohye DF, Murrell WG. 1963. The composition and structure of bacterial spores. J Cell Biol 16:579–592. https://doi.org/10.1083/jcb.16.3.579.
13. Popham DL, Bernhards CB. 2015. Spore peptidoglycan. Microbiol Spectr 3:157–177.
14. Meador-Parton J, Popham DL. 2000. Structural analysis of *Bacillus subtilis* spore peptidoglycan during sporulation. J Bacteriol 182:4491–4499. https://doi.org/10.1128/jb.182.16.4491-4499.2000.
15. Warth AD, Strominger JL. 1972. Structure of the peptidoglycan from spores of *Bacillus subtilis*. Biochemistry 11:1389–1396. https://doi.org/10.1021/bi00758a010.
16. Atrih A, Zöllner P, Allmaier G, Foster SJ. 1996. Structural analysis of *Bacillus subtilis* 168 endospore peptidoglycan and its role during differentiation. J Bacteriol 178:6173–6183. https://doi.org/10.1128/jb.178.21.6173-6183.1996.
17. Popham DL, Helin J, Costello CE, Setlow P. 1996. Analysis of the peptidoglycan structure of *Bacillus subtilis* endospores. J Bacteriol 178:6451–6458. https://doi.org/10.1128/jb.178.22.6451-6458.1996.
18. Henriques AO, Moran CP. 2007. Structure, assembly, and function of the spore surface layers. Annu Rev Microbiol 61:555–588. https://doi.org/10.1146/annurev.micro.61.080706.093224.
19. McKenney PT, Driks A, Eichenberger P. 2013. The *Bacillus subtilis* endospore: assembly and functions of the multilayered coat. Nat Rev Microbiol 11:33–44. https://doi.org/10.1038/nrmicro2921.
20. Barlass PJ, Houston CW, Clements MO, Moir A. 2002. Germination of *Bacillus cereus* spores in response to L-alanine and to inosine: the roles of *gerL* and *gerQ* operons. Microbiology 148:2089–2095. https://doi.org/10.1099/00221287-148-7-2089.
21. Swerdlow BM, Setlow B, Setlow P. 1981. Levels of H^+ and other monovalent cations in dormant and germinating spores of *Bacillus megaterium*. J Bacteriol 148:20–29.
22. Setlow B, Wahome PG, Setlow P. 2008. Release of small molecules during germination of spores of *Bacillus* species. J Bacteriol 190:4759–4763. https://doi.org/10.1128/JB.00399-08.
23. Popham DL, Helin J, Costello CE, Setlow P. 1996. Muramic lactam in peptidoglycan of *Bacillus subtilis* spores is required for spore outgrowth but not for spore dehydration or heat resistance. Proc Natl Acad Sci U S A 93:15405–15410. https://doi.org/10.1073/pnas.93.26.15405.
24. Setlow B, Melly E, Setlow P. 2001. Properties of spores of *Bacillus subtilis* blocked at an intermediate stage in spore germination. J Bacteriol 183:4894–4899. https://doi.org/10.1128/JB.183.16.4894-4899.2001.
25. Atrih A, Zöllner P, Allmaier G, Williamson MP, Foster SJ. 1998. Peptidoglycan structural dynamics during germination of *Bacillus subtilis* 168 endospores. J Bacteriol 180:4603–4612.
26. Heffron JD, Lambert EA, Sherry N, Popham DL. 2010. Contributions of four cortex lytic enzymes to germination of *Bacillus anthracis* spores. J Bacteriol 192:763–770. https://doi.org/10.1128/JB.01380-09.
27. Heffron JD, Sherry N, Popham DL. 2011. *In vitro* studies of peptidoglycan binding and hydrolysis by the *Bacillus anthracis* germination-specific lytic enzyme SleB. J Bacteriol 193:125–131. https://doi.org/10.1128/JB.00869-10.
28. Bagyan I, Setlow P. 2002. Localization of the cortex lytic enzyme CwlJ in spores of *Bacillus subtilis*. J Bacteriol 184:1219–1224. https://doi.org/10.1128/jb.184.4.1219-1224.2002.
29. Chirakkal H, O'Rourke M, Atrih A, Foster SJ, Moir A. 2002. Analysis of spore cortex lytic enzymes and related proteins in *Bacillus subtilis* endospore germination. Microbiology 148:2383–2392. https://doi.org/10.1099/00221287-148-8-2383.
30. Li Y, Butzin XY, Davis A, Setlow B, Korza G, Üstok FI, Christie G, Setlow P, Hao B. 2013. Activity and regulation of various forms of CwlJ, SleB, and YpeB proteins in degrading cortex peptidoglycan of spores of *Bacillus* species *in vitro* and during spore germination. J Bacteriol 195:2530–2540. https://doi.org/10.1128/JB.00259-13.
31. Bernhards CB, Popham DL. 2014. Role of YpeB in cortex hydrolysis during germination of *Bacillus anthracis* spores. J Bacteriol 196:3399–3409. https://doi.org/10.1128/JB.01899-14.
32. Ragkousi K, Eichenberger P, van Ooij C, Setlow P. 2003. Identification of a new gene essential for germination of *Bacillus subtilis* spores with Ca^{2+}-dipicolinate. J Bacteriol 185:2315–2329. https://doi.org/10.1128/jb.185.7.2315-2329.2003.
33. Paidhungat M, Ragkousi K, Setlow P. 2001. Genetic requirements for induction of germination of spores of *Bacillus subtilis* by Ca^{2+}-dipicolinate. J Bacteriol 183:4886–4893. https://doi.org/10.1128/JB.183.16.4886-4893.2001.
34. van Opijnen T, Bodi KL, Camilli A. 2009. Tn-seq: high-throughput parallel sequencing for fitness and genetic interaction studies in microorganisms. Nat Methods 6:767–772. https://doi.org/10.1038/nmeth.1377.
35. McKenney PT, Eichenberger P. 2012. Dynamics of spore coat morphogenesis in *Bacillus subtilis*. Mol Microbiol 83:245–260. https://doi.org/10.1111/j.1365-2958.2011.07936.x.
36. Lombard V, Golaconda Ramulu H, Drula E, Coutinho PM, Henrissat B. 2014. The carbohydrate-active enzymes database (CAZy) in 2013. Nucleic Acids Res 42:D490–D495. https://doi.org/10.1093/nar/gkt1178.
37. Abecasis AB, Serrano M, Alves R, Quintais L, Pereira-Leal JB, Henriques AO. 2013. A genomic signature and the identification of new sporulation genes. J Bacteriol 195:2101–2115. https://doi.org/10.1128/JB.02110-12.
38. Traag BA, Pugliese A, Eisen JA, Losick R. 2013. Gene conservation among endospore-forming bacteria reveals additional sporulation genes in *Bacillus subtilis*. J Bacteriol 195:253–260. https://doi.org/10.1128/JB.01778-12.
39. Ozin AJ, Henriques AO, Yi H, Moran CP. 2000. Morphogenetic proteins SpoVID and SafA form a complex during assembly of the *Bacillus subtilis* spore coat. J Bacteriol 182:1828–1833. https://doi.org/10.1128/jb.182.7.1828-1833.2000.
40. Keynan A, Halvorson HO. 1962. Calcium dipicolinic acid-induced germination of *Bacillus cereus* spores. J Bacteriol 83:100–105.
41. Blair DE, Schüttelkopf AW, MacRae JI, van Aalten D. 2005. Structure and metal-dependent mechanism of peptidoglycan deacetylase, a streptococcal virulence factor. Proc Natl Acad Sci U S A 102:15429–15434. https://doi.org/10.1073/pnas.0504339102.
42. Psylinakis E, Boneca IG, Mavromatis K, Deli A, Hayhurst E, Foster SJ, Vårum KM, Bouriotis V. 2005. Peptidoglycan N-acetylglucosamine deacetylases from *Bacillus cereus*, highly conserved proteins in *Bacillus anthracis*. J Biol Chem 280:30856–30863. https://doi.org/10.1074/jbc.M407426200.
43. Rosen DL, Sharpless C, McGown LM. 1997. Bacterial spore detection and determination by use of terbium dipicolinate photoluminescence. Anal Chem 69:1082–1085. https://doi.org/10.1021/ac960939w.
44. Yi X, Setlow P. 2010. Studies of the commitment step in the germination of spores of *Bacillus* species. J Bacteriol 192:3424–3433. https://doi.org/10.1128/JB.00326-10.
45. Kuwana R, Kasahara Y, Fujibayashi M, Takamatsu H, Ogasawara N, Watabe K. 2002. Proteomics characterization of novel spore proteins of *Bacillus subtilis*. Microbiology 148:3971–3982. https://doi.org/10.1099/00221287-148-12-3971.
46. Lai E-M, Phadke ND, Kachman MT, Giorno R, Vazquez S, Vazquez JA, Maddock JR, Driks A. 2003. Proteomic analysis of the spore coats of *Bacillus subtilis* and *Bacillus anthracis*. J Bacteriol 185:1443–1454. https://doi.org/10.1128/jb.185.4.1443-1454.2003.
47. Kim H, Hahn M, Grabowski P, McPherson DC, Otte MM, Wang R, Ferguson CC, Eichenberger P, Driks A. 2006. The *Bacillus subtilis* spore coat protein interaction network. Mol Microbiol 59:487–502. https://doi.org/10.1111/j.1365-2958.2005.04968.x.
48. Abhyankar W, Beek AT, Dekker H, Kort R, Brul S, Koster CG. 2011. Gel-free proteomic identification of the *Bacillus subtilis* insoluble spore coat

protein fraction. Proteomics 11:4541–4550. https://doi.org/10.1002/pmic.201100003.
49. Abhyankar W, Hossain AH, Djajasaputra A, Permpoonpattana P, Beek AT, Dekker HL, Cutting SM, Brul S, Koning LJ, Koster CG. 2013. In pursuit of protein targets: proteomic characterization of bacterial spore outer layers. J Proteome Res 12:4507–4521. https://doi.org/10.1021/pr4005629.
50. Nielsen H, Engelbrecht J, Brunak S, Heijne von G. 1997. Identification of prokaryotic and eukaryotic signal peptides and prediction of their cleavage sites. Protein Eng 10:1–6. https://doi.org/10.1093/protein/10.1.1.
51. Almagro Armenteros JJ, Tsirigos KD, Sønderby CK, Petersen TN, Winther O, Brunak S, Heijne von G, Nielsen H. 2019. SignalP 5.0 improves signal peptide predictions using deep neural networks. Nat Biotechnol 37:420–423. https://doi.org/10.1038/s41587-019-0036-z.
52. Fukushima T, Yamamoto H, Atrih A, Foster SJ, Sekiguchi J. 2002. A polysaccharide deacetylase gene (*pdaA*) is required for germination and for production of muramic delta-lactam residues in the spore cortex of *Bacillus subtilis*. J Bacteriol 184:6007–6015. https://doi.org/10.1128/jb.184.21.6007-6015.2002.
53. Bartels J, Blüher A, López Castellanos S, Richter M, Günther M, Mascher T. 2019. The *Bacillus subtilis* endospore crust: protein interaction network, architecture and glycosylation state of a potential glycoprotein layer. Mol Microbiol 112:1576–1592. https://doi.org/10.1111/mmi.14381.
54. Zeigler DR, Prágai Z, Rodriguez S, Chevreux B, Muffler A, Albert T, Bai R, Wyss M, Perkins JB. 2008. The origins of 168, W23, and other *Bacillus subtilis* legacy strains. J Bacteriol 190:6983–6995. https://doi.org/10.1128/JB.00722-08.
55. Sterlini JM, Mandelstam J. 1969. Commitment to sporulation in *Bacillus subtilis* and its relationship to development of actinomycin resistance. Biochem J 113:29–37. https://doi.org/10.1042/bj1130029.
56. Koo B-M, Kritikos G, Farelli JD, Todor H, Tong K, Kimsey H, Wapinski I, Galardini M, Cabal A, Peters JM, Hachmann A-B, Rudner DZ, Allen KN, Typas A, Gross CA. 2017. Construction and analysis of two genome-scale deletion libraries for *Bacillus subtilis*. Cell Syst 4:291–305.e7. https://doi.org/10.1016/j.cels.2016.12.013.
57. Gibson DG. 2011. Enzymatic assembly of overlapping DNA fragments. Methods Enzymol 498:349–361. https://doi.org/10.1016/B978-0-12-385120-8.00015-2.
58. Meeske AJ, Sham L-T, Kimsey H, Koo B-M, Gross CA, Bernhardt TG, Rudner DZ. 2015. MurJ and a novel lipid II flippase are required for cell wall biogenesis in *Bacillus subtilis*. Proc Natl Acad Sci U S A 112:6437–6442. https://doi.org/10.1073/pnas.1504967112.
59. Carver T, Harris SR, Berriman M, Parkhill J, McQuillan JA. 2012. Artemis: an integrated platform for visualization and analysis of high-throughput sequence-based experimental data. Bioinformatics 28:464–469. https://doi.org/10.1093/bioinformatics/btr703.
60. Doan T, Marquis KA, Rudner DZ. 2005. Subcellular localization of a sporulation membrane protein is achieved through a network of interactions along and across the septum. Mol Microbiol 55:1767–1781. https://doi.org/10.1111/j.1365-2958.2005.04501.x.
61. Morlot C, Uehara T, Marquis KA, Bernhardt TG, Rudner DZ. 2010. A highly coordinated cell wall degradation machine governs spore morphogenesis in *Bacillus subtilis*. Genes Dev 24:411–422. https://doi.org/10.1101/gad.1878110.
62. Fujita M. 2000. Temporal and selective association of multiple sigma factors with RNA polymerase during sporulation in *Bacillus subtilis*. Genes Cells 5:79–88. https://doi.org/10.1046/j.1365-2443.2000.00307.x.
63. Jacquier N, Yadav AK, Pillonel T, Viollier PH, Cava F, Greub G, Jacquier N, Yadav AK, Pillonel T, Viollier PH, Cava F, Greub G. 2019. A SpoIID homolog cleaves glycan strands at the chlamydial division septum. mBio 10:e01128-19. https://doi.org/10.1128/mBio.01128-19.